3D displacement measurements of the tympanic membrane with digital holographic interferometry

S. Muñoz Solís,* F. Mendoza Santoyo, and M. del Socorro Hernández-Montes

Centro de Investigaciones en Óptica, A.C., Loma del Bosque 115, León, Guanajuato, 37150, Mexico
*smsolis@cio.mx

Abstract: A digital holographic interferometry (DHI) system with three object-illumination beams is used for the first time to measure micro-deformations along the x, y and z axes (3D) on the tympanic membrane (TM) surface of a post-mortem cat. In order to completely and accurately measure the TM surface displacements its shape is required to map on it the x, y and z micro-deformations. The surface contour is obtained by applying small shifts to the object illumination source position. A cw laser in stroboscopic mode and a CCD camera were used and synchronized to the acoustic excitation wave that produces a resonant vibration mode on the tympanic membrane surface. This research work reports on the 3D full field of view response of the TM to sound pressure, and has as its main goal the presentation of DHI as an alternative technique to study the TM real displacement behavior when subjected to sound waves, so it can be used as a diagnostic tool to prevent and treat TM diseases.

OCIS codes: (120.2880) Holographic interferometry; (120.4630) Optical inspection; (170.6935) Tissue characterization; (120.5050) Phase measurement.

References and links

1. G. Volandri, F. Di Puccio, P. Forte, and C. Carmignani, "Biomechanics of the tympanic membrane," J. Biomech. **44**(7), 1219–1236 (2011).
2. S. M. Khanna and J. Tonndorf, "Tympanic membrane vibrations in cats studied by time-averaged holography," J. Acoust. Soc. Am. **51**(6B), 1904–1920 (1972).
3. J. Tonndorf and S. M. Khanna, "The role of the tympanic membrane in middle ear transmission," Ann. Otol. Rhinol. Laryngol. **79**(4), 743–753 (1970).
4. J. Tonndorf and S. M. Khanna, "Tympanic-membrane vibrations in human cadaver ears studied by time-averaged holography," J. Acoust. Soc. Am. **52**(4B), 1221–1233 (1972).
5. M. K. Kim, "Applications of Digital Holography in Biomedical Microscopy," J. Opt. Soc. Korea **14**(2), 77–89 (2010).
6. C. M. Vest, *Holographic Interferometry* (John Wiley & Sons, 1979).
7. G. Pedrini, W. Osten, and M. E. Gusev, "High-speed digital holographic interferometry for vibration measurement," Appl. Opt. **45**(15), 3456–3462 (2006).
8. P. K. Rastogi, "Principles of holographic interferometry and speckle metrology," Top. Appl. Phys. **77**, 103–151 (2000).
9. M. del Socorro Hernández-Montes, C. Pérez-López, and F. Mendoza, "Finding the position of tumor inhomogeneities in a gel-like model of a human breast using 3-D pulsed digital holography," J. Biomed. Opt. **12**, 1–5 (2007).
10. D. D. Aguayo, F. Mendoza Santoyo, M. H. De la Torre-I, M. D. Salas-Araiza, C. Caloca-Mendez, and D. A. Gutierrez Hernandez, "Insect wing deformation measurements using high speed digital holographic interferometry," Opt. Express **18**(6), 5661–5667 (2010).
11. F. M. Santoyo, G. Pedrini, S. Schedin, and H. J. Tiziani, "3D displacement measurements of vibrating objects with multi-pulse digital holography," Meas. Sci. Technol. **10**(12), 1305–1308 (1999).
12. S. Schedin, G. Pedrini, H. J. Tiziani, and F. M. Santoyo, "Simultaneous three-dimensional dynamic deformation measurements with pulsed digital holography," Appl. Opt. **38**(34), 7056–7062 (1999).
13. G. Pedrini, S. Schedin1, and H. J. Tiziani, "Pulsed digital holography combined with laser vibrometry for 3D measurements of vibrating objects," Opt. Lasers Eng. **38**, 117–129 (2002).
14. M. De la Torre-Ibarra, F. Mendoza-Santoyo, C. Pérez-López, and S. A. Tonatiuh, "Detection of surface strain by three-dimensional digital holography," Appl. Opt. **44**(1), 27–31 (2005).

#160352 - $15.00 USD Received 20 Dec 2011; revised 2 Feb 2012; accepted 6 Feb 2012; published 22 Feb 2012

15. M. Takeda, H. Ina, and S. Kobayashi, "Fourier-transform method of fringe-pattern analysis for computer-based topography and Interferometry," J. Opt. Soc. Am. **72**(1), 156–160 (1982).
16. C. Quan, W. Chen, and C. J. Tay, "Shape measurement by multi-illumination method in digital holographic Interferometry," Opt. Commun. **281**(15-16), 3957–3964 (2008).
17. U. Schnars and W. Jueptner, *Digital Holography: Digital Hologram Recording Numerical Reconstruction, and Related Techniques* (Springer, 2005).
18. I. Yamaguchi, S. Ohta, and J.-I. Kato, "Surface contouring by phase-shifting digital holography," Opt. Lasers Eng. **36**(5), 417–428 (2001).
19. J. J. J. Dirckx and W. F. Decraemer, "Interferometer for eardrum shape measurement, based on projection of straight line rulings," Lasers Med. Sci. **15**(2), 131–139 (2000).
20. W. F. Decraemer and W. R. J. Funnell, "Anatomical and mechanical properties of the tympanic membrane," In: B. Ars, editor. Chronic otitis media. Pathogenesis-oriented therapeutic Management. The Haugue: Kugler, 51–84 (2008).
21. C. Furlong, J. J. Rosowski, N. Hulli, and M. E. Ravicz, "Preliminary analyses of tympanic-membrane motion from holographic measurements," Strain **45**(3), 301–309 (2009).
22. M. del Socorro Hernández-Montes, C. Furlong, J. J. Rosowski, N. Hulli, E. Harrington, J. T. Cheng, M. E. Ravicz, and F. M. Santoyo, "Optoelectronic holographic otoscope for measurement of nano-displacements in tympanic membranes," J. Biomed. Opt. **14**(3), 034023 (2009).
23. J. J. Rosowski, J. T. Cheng, M. E. Ravicz, N. Hulli, M. Hernandez-Montes, E. Harrington, and C. Furlong, "Computer-assisted time-averaged holograms of the motion of the surface of the mammalian tympanic membrane with sound stimuli of 0.4-25 kHz," Hear. Res. **253**(1-2), 83–96 (2009).
24. M. S. Hernández-Montes, F. Mendoza Santoyo, C. Pérez López, S. Muñoz Solís, and J. Esquivel, "Digital holographic interferometry applied to the study of tympanic membrane displacements," Opt. Lasers Eng. **49**(6), 698–702 (2011).

1. Introduction

The importance of an accurate clinical diagnostic of the tympanic membrane health condition is of great interest in medicine and related fields. Due to its location within the human auditory apparatus researchers have developed highly specialized techniques and tools to study and analyze the TM rather complex structure, so much in recent studies [1] as in previous years [2–4].The use of optical non-invasive techniques are becoming increasingly important in medicine due to their capability of performing full-field of view measurements, with data acquisition, interpretation and display done within a few seconds [5]. In particular DHI has proven to have the ability to study qualitatively and quantitatively 3D deformations in solid and elastic materials, and biological samples [6–10], amongst many other applications. Measurements are done from phase maps that contain amplitude and phase information directly related to the object deformation. In order to have a complete and accurate description of the object deformation, its surface shape (contour) must be found so that the amplitude and phase (direction of object motion) can be mapped on the object's surface. An object's shape may be found using a wide variety of techniques and instrumentation, it is a most required information in many fields. From a contour map the object's topographic characteristics are obtained and applied in areas such as on-line inspection, medical diagnostics, industrial/mechanical design, optical surface inspection, etc.

In this paper an application of 3D-DHI to measure TM surface deformation values is presented, with its main contribution being the capacity to separate the deformation in the x, y and z displacement components that may be combined to obtain information regarding the TM surface tangential and normal displacements. The x, y and z data must be mapped with a direct relationship to the TM surface, i.e., 3D displacement information needs to be located on a point-to-point basis over its corresponding position on the surface. For this purpose the TM contour is measured using two (out of three) object source illumination positions, and the shape is obtained from the phase difference obtained from these two illumination positions [11–14]. Thus, with the same optical set-up an accurate description of the 3D TM displacement data is achieved. The results stem from experimental tests carried out on a fresh cat's post-mortem tympanic membrane at a resonating frequency of 1.2 kHz.

2. Determination of tympanic membrane displacements in 3d

The optical set-up, consists of three different illumination directions for the object, where each direction of object illumination is represented by a unit sensitivity vector, as shown in

#160352 - $15.00 USD Received 20 Dec 2011; revised 2 Feb 2012; accepted 6 Feb 2012; published 22 Feb 2012

Fig. 1, used to measure the object displacements along the x, y and z coordinate axes. The TM sample is stimulated with sound waves and illuminated with a Verdi laser at 532 nm. An acousto-optic modulator is placed near the laser in order to produce stroboscopic light, where the first order diffracted beam is used. The laser beam is thus divided into two beams using a 50:50 beam splitter, one of them is coupled into a single mode optical fiber and serves as the reference beam, while the other beam is also coupled into an optical fiber which may be moved and placed on its corresponding optical mount located in three different positions-directions of object illumination. The versatility to use optical fibers in the setup is shown in the easiness to place them for different illumination positions. The backscattered light from the object is then collected by a doublet lens with 30mm focal length placed at 5 cm from the CCD camera sensor. The 50:50 beam combiner placed in front of CCD sensor serves to bring together the reference and object beams whose overlap form the digital holographic interferograms (dhi, or holograms henceforth) which are recorded individually for each illumination direction. To avoid saturation of the CCD sensor, the beam intensity was measured to give a good contrast in the interference pattern: this was achieved by decoupling the reference beam from the fiber interface. External trigger pulses from a pulse generator are used to synchronize the hologram acquisition with the sound wave excitation signal and to handle the drive of the acoustic-optic modulator. Two holograms are captured, one hologram is recorded in a base state without any sound signal (signal excitation phase at ~0°) and the other at the sound wave maximum amplitude (signal excitation phase at ~90°).

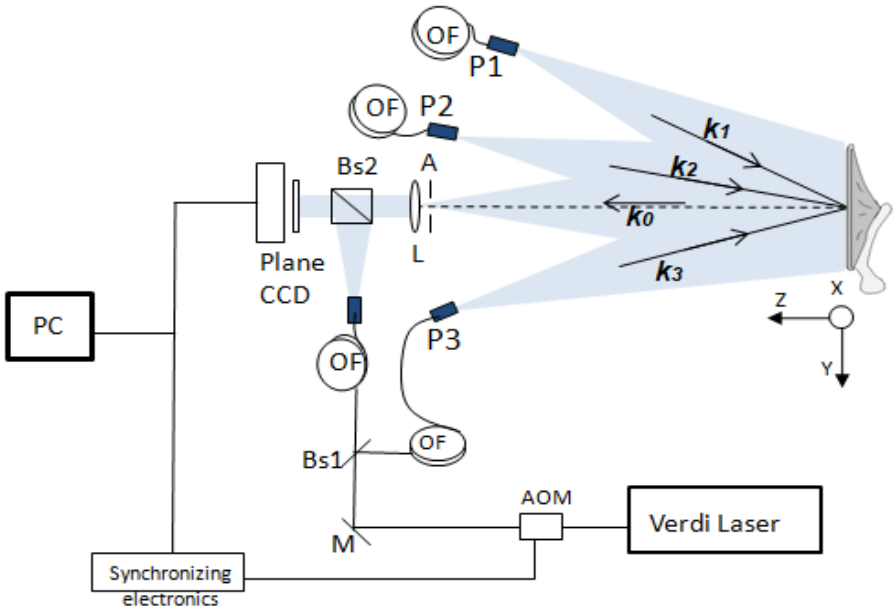

Fig. 1. 3D-DHI experimental setup: M, Mirror; Bs1, beam splitter, Bs2, beam combiner; L, lens; A, aperture; OF, single mode optical fiber; AOM, acousto-optic modulators; P1, P2, P3, object illumination directions.

Mathematically DHI may be described as follows: the CCD camera sensor receives an amount of light proportional to the field intensity produced by the interference between the object and reference beams, where the intensity at any point I(x,y) can be written as,

$$I_{1,2}(x,y)=I_o(x,y)+I_r(x,y)+2\sqrt{I_o I_r}\cos(\varphi+\psi) \qquad (1)$$

where I_o and I_r are the intensities due to object and reference beams respectively, ψ denotes the randomness of the speckle field coming from the object, and the additional phase

#160352 - $15.00 USD Received 20 Dec 2011; revised 2 Feb 2012; accepted 6 Feb 2012; published 22 Feb 2012

difference φ represents the object surface displacement. The phase between any two object positions is obtained from the Fourier-transform method [15].

$$\Delta\varphi(x,y)=\arctan\frac{\mathrm{Re}\{I_1(x,y)\}\,\mathrm{Im}\{I_2(x,y)\}-\mathrm{Re}\{I_2(x,y)\}\,\mathrm{Im}\{I_1(x,y)\}}{\mathrm{Im}\{I_1(x,y)\}\,\mathrm{Im}\{I_2(x,y)\}+\mathrm{Re}\{I_1(x,y)\}\,\mathrm{Re}\{I_2(x,y)\}} \qquad (2)$$

where $\Delta\varphi(x,y)$ is the desired phase map of the hologram pair, Re and Im represent the real and imaginary part of a complex number. The wrapped phase maps are unwrapped using a minimum cost matching algorithm from Phase Vision Ltd. Pv_psua2.

Subtracting the holograms obtained between two object states results in a phase map that contains the information about the displacement undergone from one position to the next. The sensitivity vectors of the optical arrangement is determined by the object illumination and observation directions as given by the geometry of the setup. In Fig. 1 the object illumination directions are denoted with the unit vectors k_1, k_2 and k_3. The observation direction is denoted with the unit vector k_0. The sensitivity vectors are given by $s_i = k_i - k_0$ i=1,2,3 . To find the x, y and z (3D) object displacement it is required to combine the resultant of the sensitivity vectors obtained from the setup for each unitary vector with the individual phases and the object contour. The relationship of the phase difference with each displacement vector is determined by:

$$\begin{pmatrix} d_x \\ d_y \\ d_z \end{pmatrix} = \frac{\lambda}{2\pi}\begin{bmatrix} S_{1x} & S_{1y} & S_{1z} \\ S_{2x} & S_{2y} & S_{2z} \\ S_{3x} & S_{3y} & S_{3z} \end{bmatrix}^{-1}\begin{bmatrix} \Delta\varphi_1 \\ \Delta\varphi_2 \\ \Delta\varphi_3 \end{bmatrix} \qquad (3)$$

where d_x, d_y and d_z, are the components of deformation and λ is the wavelength of the laser light. $\Delta\varphi_{n\ n=1,2,3}$ is the resulting phase for each position of illumination. The sensitivity vectors and phase maps are known from the experiment and the Eq. (3) may be readily solved to find the x, y and z displacements, which are combined with the shape of the object in order to obtain a complete 3D representation of the object deformation.

The optical arrangement used to determine the 3D contour is the same as that shown in Fig. 1, however for shape measurement the object holograms are taken while it is at rest: the shape of the tympanic membrane is found using the method that uses two-illumination positions [16,17], such that two holograms are recorded of the same surface illuminated from different positions, using only one arm of the interferometer. The optimum illumination directions are usually determined by a trade-off between the maximum sensitivity and minimum projected shadows in the reconstructed image.

The angle θ is measured from the fixed illumination position to the normal axis to the camera sensor k_0. The angular displacement given to one of the illumination sources is performed by slightly displacing one source with respect to the other using a micrometric screw. With these data the object surface height-change $h(x)$ [18] may be found from the difference between the reconstructed phases which are recorded before and after the small tilt $\Delta\theta$ of the object illuminating beam.

$$\Delta\varphi = 2K\sin\frac{\Delta\theta}{2}\left[x\cos\left(\theta+\frac{\Delta\theta}{2}\right)-h(x)\sin\theta+\frac{\Delta\theta}{2}\right] \qquad (4)$$

It has been found that the TM has a conical shape [19] with its apex pointing approximately straight inward. The size and shape are variable from one sample to another. Figure 2 shows the tympanic membrane shape found. To measure its depth, the umbo is considered as the reference point with respect to the tympanic annulus plane: a depth of 2 mm

#160352 - $15.00 USD Received 20 Dec 2011; revised 2 Feb 2012; accepted 6 Feb 2012; published 22 Feb 2012

was found using Eq. (4), which is good agreement with values found elsewhere [20]. From this figure it can be observed surrounding bone residuals that could not be removed in its entirety belonging to the tympanic cavity overhanging at the edge of the TM, right above the tympanic annulus.

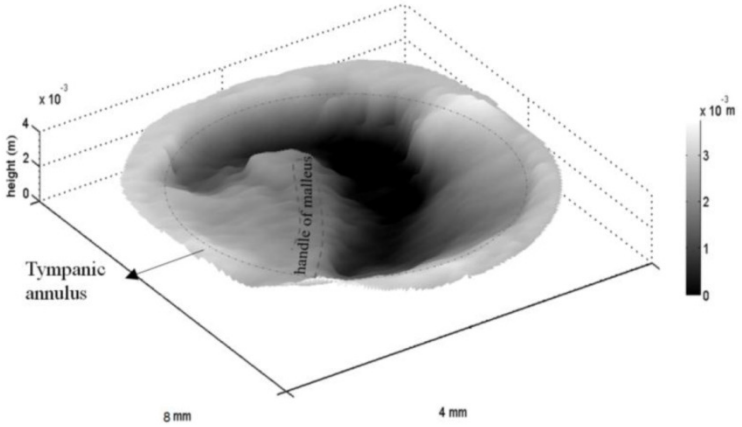

Fig. 2. Experimentally found TM surface contour.

3. Preparation of the sample

For the present study the animal selected was a homeless cat, kept in an animal shelter and due to put to sleep. The sample preparation consisted of the separation of the head after the euthanasia. Cuttings were made in the external auditory canal to ensure visual access to the tympanic membrane surface of roughly 90%, leaving the tympanic membrane and ossicles (malleus, incus and stapes) intact as well as tendons and ligaments that support it. The sample was preserved using a saline solution, wrapped in a gauze and placed in a freezer. Before experimenting on the sample, it is thawed in a saline solution at room temperature. The tympanic membrane was slightly sprayed with a white color developer in order to obtain larger light backscattered from its surface, ensuring that the membrane was not damaged or lost its elastic properties. The tympanic membrane had an area of approximately 8 mm x 4 mm. These data varies according to race, age, sex, as well as any abnormal pathology that the cat could have had.

Several studies have shown that the middle ear can remain relatively normal for long periods of time, or even days after death, as reported Khanna and Tonndorf [2] in cats. where the acoustic properties of the tympanic membrane show no significant difference on after death samples, i.e., there is no significant change in their mode of vibration for low-frequencies. The study of the tympanic membrane in this work was carried out in fresh cadaver heads. In the measurements, the area of interest was kept moist with a saline solution to prevent the tympanic membrane drying out.

4. Results

The images are recorded sequentially with a CCD camera of 1392x1024 pixels at 12 bits dynamic range, i.e. a pair of holograms in each direction of illumination. The sample was excited with a loudspeaker which is controlled by a function generator, and synchronized with the camera. The identification of resonant vibration modes consisted in the measuring of frequency response of the tympanic membrane to acoustic stimuli in the range of 500 Hz to 15 kHz. The patterns found in these frequencies were reported in references [21–24]. From this analysis, the mode of vibration at 1.2 kHz was chosen because renders simple vibration patterns and the whole TM vibrates almost in phase.

The unwrapped phase maps along the three sensitivity vectors are shown in Fig. 3 and are used to evaluate the sample surface x, y and z displacement, using Eq. (3). In addition since

#160352 - $15.00 USD Received 20 Dec 2011; revised 2 Feb 2012; accepted 6 Feb 2012; published 22 Feb 2012

the shape of the TM is known, the normal and tangential components of the deformation of the tympanic membrane are calculated. Figure 4 shows the x, y and z deformation superimposed on the TM surface contour. As expected from the TM position in the inner ear and to the fact that it was excited by acoustic pressure predominantly travelling along the z direction, the observed maximum vibration amplitude is in this direction. Figure 5 shows the results for the normal to the surface and the vector representation of the tangential (x and y combined) to the surface overlaid on the TM contour data found. The larger deformation is along the normal direction [Fig. 5(A)] and its amplitude resembles that of the z direction. The tangential deformation seems to have a circular direction in some regions of the TM, a feature that may comply to the particular resonant mode energy conservation [Fig. 5(B)], apart from the fact that the x and y displacement values are rather small as compare to those in the z direction. The vectors on the surface are unitary, and their perspective may appear to be larger in some areas.

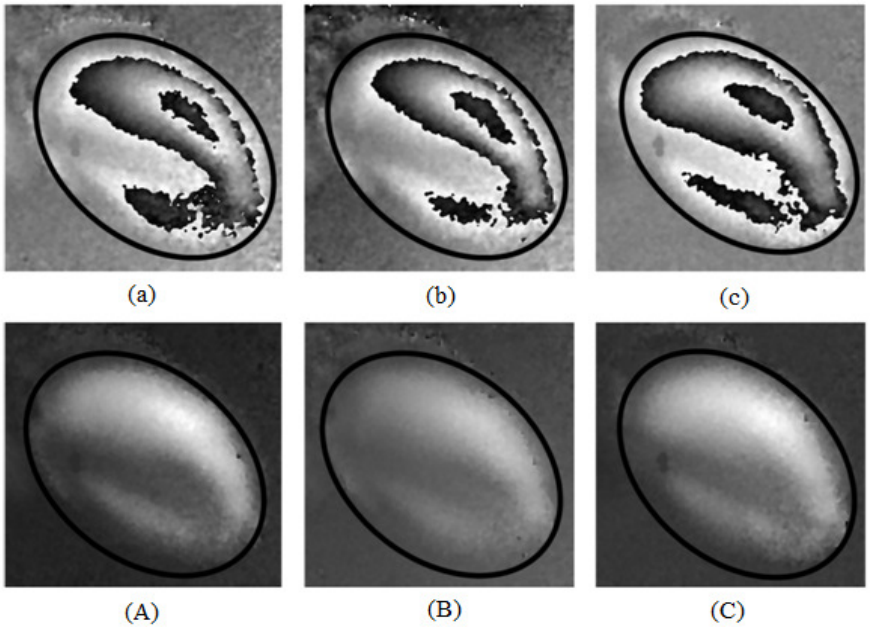

Fig. 3. Measurement of the membrane vibration at 1.2 kHz. (a), (b) and (c) are wrapped phase maps corresponding to the illumination directions $\mathbf{k}_1$, $\mathbf{k}_2$ and $\mathbf{k}_3$, respectively (see Fig. 1). The unwrapped phase maps (A), (B) and (C) were obtained from previous phase maps.

#160352 - $15.00 USD Received 20 Dec 2011; revised 2 Feb 2012; accepted 6 Feb 2012; published 22 Feb 2012

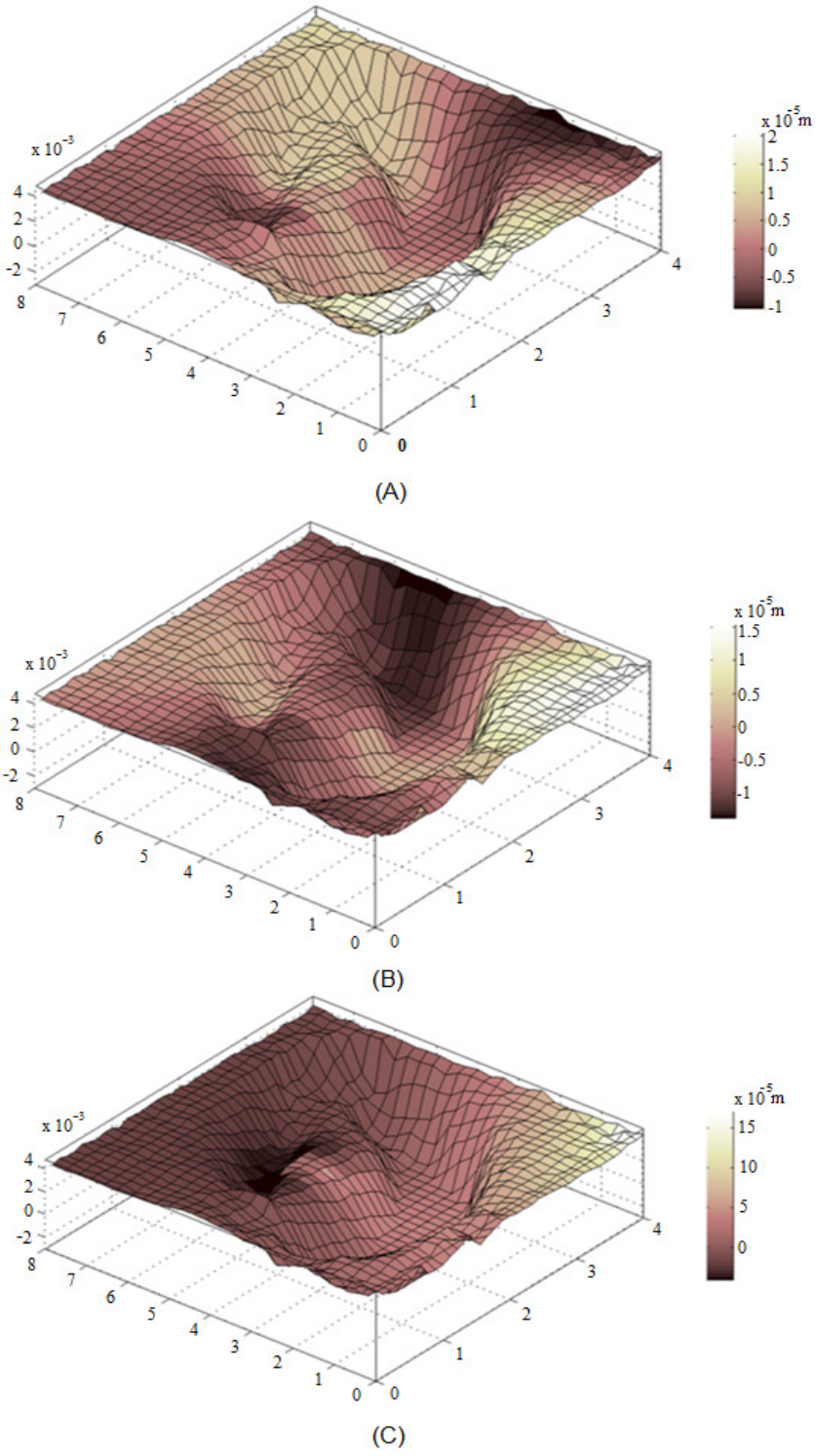

Fig. 4. Displacements along x, y and z directions on TM (A), (B), and (C), respectively. The shape of the object is given in mm. The color bar scale is different for each picture and vibration amplitude is in μm.

#160352 - $15.00 USD Received 20 Dec 2011; revised 2 Feb 2012; accepted 6 Feb 2012; published 22 Feb 2012

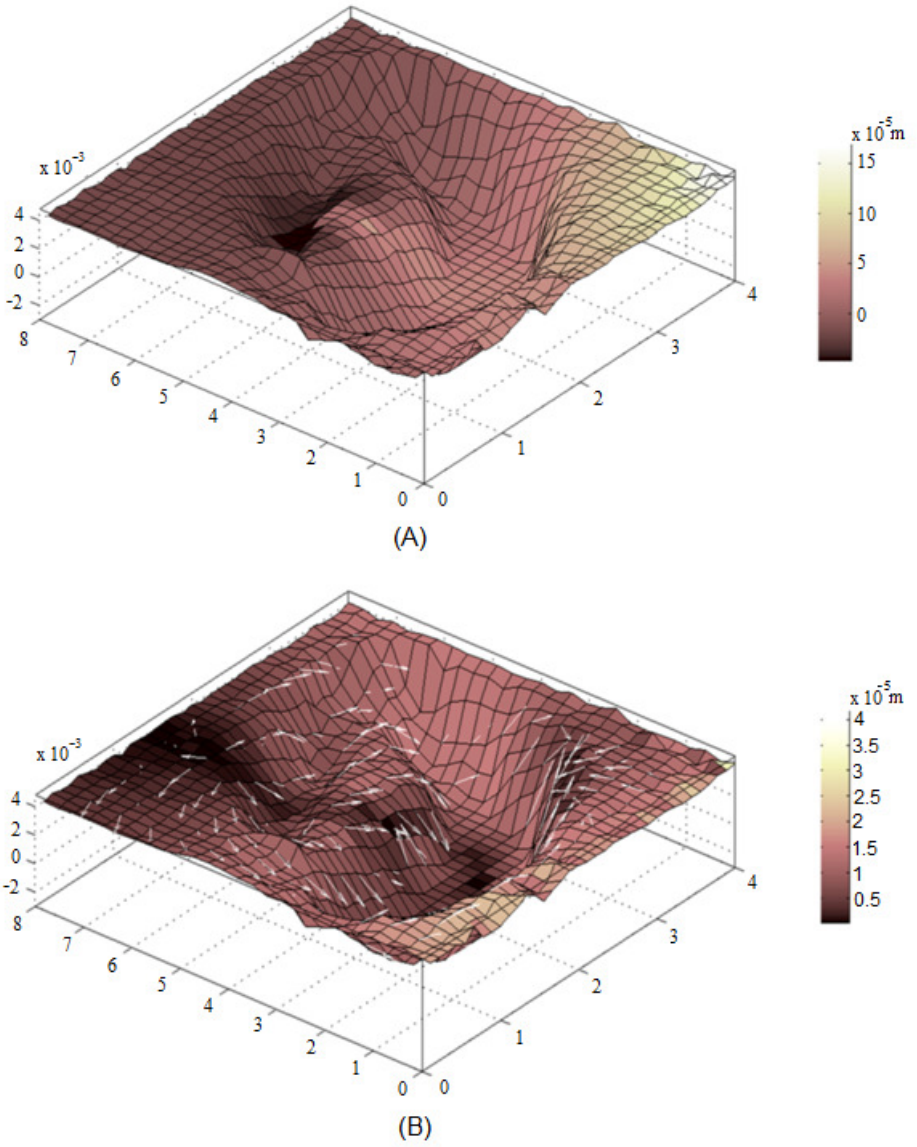

Fig. 5. Deformation overlaid on the tympanic membrane contour, in (A) the normal direction, and (B) the tangential direction.

5. Conclusions

3D Digital Holographic Interferometry was employed to measure from three different illumination directions the dynamic displacement of the tympanic membrane. In order to accurately and completely determine the TM deformation the shape of the sample was experimentally obtained and found to have an almost conical shape, as predicted by naked eye observations. The cat's TM depth was estimated about two millimeters with respect to the umbo, value slightly higher, about 9%, than the one reported in previous work, this is probably due to typical physiology variations between the samples. The advantage of using 3D DHI in comparison with the more traditional and easy to set 1D optical configuration is that the three displacement components are separated from each other, so individual displacement maps for the three directions can be calculated and overlaid with the object

#160352 - $15.00 USD Received 20 Dec 2011; revised 2 Feb 2012; accepted 6 Feb 2012; published 22 Feb 2012

shape. Since the displacement components are individually found the tangential and normal TM displacements may be calculated, a new contribution and thus an advantage in relation to conventional methods.

3D DHI is able to describe qualitatively and quantitatively the displacement components on the TM surface with sub-micrometric resolution. The optical setup used has great versatility in its manipulation with the use of optical fibers and therefore this interferometric arrangement may be implemented in a system of easy use and hence ready to be transferred for medical research to study and examine the TMs in live animals and humans under diverse conditions.

The 3D data combined with the TM surface contour should bring new improvements in the understanding of the TM surface motion, a fact that no doubt will contribute to enhance the knowledge and clarify the complex function of this important tissue.

From the results obtained we can safely say that the interference patterns found are repetitive, independently if the measurement of tympanic membrane was conducted in fresh cadaver heads or days after death.

Acknowledgments

The authors would like to acknowledge partial financial support from CONACYT (Consejo Nacional de Ciencia y Tecnología, México) through project 42971.

#160352 - $15.00 USD Received 20 Dec 2011; revised 2 Feb 2012; accepted 6 Feb 2012; published 22 Feb 2012